TRANSACTIONS ON ELECTRICAL AND ELECTRONIC MATERIALS
Vol. 18, No. 4, pp. 190-194, August 25, 2017

Regular Paper

pISSN: 1229-7607 eISSN: 2092-7592
DOI: https://doi.org/10.4313/TEEM.2017.18.4.190
OAK Central: http://central.oak.go.kr

Leakage Current Energy Harvesting Application in a Photovoltaic (PV) Panel Transformerless Inverter System

Md. Noman Habib Khan†
School of Electrical and Data Engineering, Faculty of Engineering and Information Technology, University Technology of Sydney, New South Wales 2007, Australia

Sheroz Khan
Department of Electrical and Computer Engineering, International Islamic University Malaysia, Kuala Lumpur 50728, Malaysia

Received March 17, 2016; Revised March 24, 2017; Accepted March 26, 2017

Present-day solar panels incorporate inverters as their core components. Switching devices driven by specialized power controllers are operated in a transformerless inverter topology. However, some challenges associated with this configuration include the absence of isolation, causing leakage currents to flow through various components toward ground. This inevitably causes power losses, often being also the primary reason for the power inverters' analog equipment failure. In this paper, various aspects of the leakage currents are studied using different circuit analysis methods. The primary objective is to convert the leakage current energy into a usable DC voltage source. The research is focused on harvesting the leakage currents for producing circa 1.1 V, derived from recently developed rectifier circuits, and driving a 200 Ω load with a power in the milliwatt range. Even though the output voltage level is low, the harvested power could be used for charging small batteries or capacitors, even driving light loads.

Keywords : Photovoltaic (PV) panel, Leakage current (LC), Power inverter, Low pass filter (LPF), Rectifier, Summation circuit, Flyback converter

1. INTRODUCTION

Photovoltaic (PV) panels are becoming widely used as the installation volumes rise and the achievable power per PV module increases. Moreover, an affordable price as well as high efficiency and pollution-free technology expand their usability in the renewable energy generation field [1,2]. The most expensive component of a PV system has traditionally been the inverter. However, the inverters' prices decreased considerably over the recent years, leading to an increase in the PV systems' energy production capacity [3]. The PV module output voltage is only filtered before being used for local consumption. However, for transmission to remote locations, in most cases, it needs be converted to AC using grid-tied inverters. Reduced inverters' cost will definitely result in a large-scale adoption of solar panels, replacing nuclear power generation associated with the risks of plant disasters, as it recently happened in Japan [4]. Moreover, solar panels have been proven effective for electricity generation in powering an Oxyhydrogen (HHO) generator used in the combustion chamber of vehicles' engine for boosting its fuel mixture and reducing fuel consumption [5]. This technology has been under thorough evaluation for usage in residential PV systems installations as well as for industrial developments in the Indo-Pakistan-Bangladesh sub-continent, which is currently suffering a shortage in electrical power generation. The DC PV panels' output is fed to the AC grid using power switching transformerless topologies such as the Z-source inverter (ZSI) and switched boost inverter (SBI) [6,7]. Although exhibiting a reduced overall cost and size,

† Author to whom all correspondence should be addressed:
E-mail: nomanxp76@gmail.com

such transformerless configurations suffer from the inherent issue of leakage current. The reduction of the leakage current has been a design goal, not only primarily for safety reasons, but also to reduce power losses, as discussed in recent work related to topologies like the PWM with zero voltage switching (ZVS) [8–10]. Leakage current minimization is also being addressed in the IC design, as in the power gating technique, CMOS design technique, reverse back bias (RBB) technique, Dual-Vt and Dual-Tox, bit line leakage current compensation technique, etc. [9–12]. In order to use a PV panel for charging different electronic devices such as laptops or mobile phones for a longer battery lifetime, the leakage current is the main concern [13]. Recently, the researchers invest significant efforts to minimize the power losses and cost of the grid-tied solar systems [14–19]. Although small in magnitude, the leakage current occurring at different nodes of the conversion circuitry has become one of the reasons for lower power efficiency. Efforts are underway for developing traction applications using a transformerless rectifier configuration for generating a DC voltage from a fluctuating AC signal [20,21] performing the front-end rectification based on a pulse width-modulation (PWM) driven H-bridge buck rectifier. However, [22–24] discuss two useful switching rectifier MOSFET-based circuits: the fully cross coupled and gate cross coupled topologies. The maximum output voltage and efficiency obtained are presented for the conditions of highly fluctuating leakage currents converted to a DC voltage source for battery charging purposes or powering small LEDs for signaling. Harvesting of such leakage currents with gate cross-coupled and fully cross-coupled configurations and converting the energy into a usable DC supply is the focus of work in this paper.

2. BLOCK DIAGRAM AND CIRCUIT DESCRIPTION

Transformer-based inverters are less commonly used nowadays due to some limitations, while the transformerless configuration is a widely employed inverter topology, using a large variety of devices for a convenient electric power transfer to the grid with high efficiency.

Figure 1 shows the system block diagram comprising a 12 V PV panel sourcing power to a transformerless inverter.

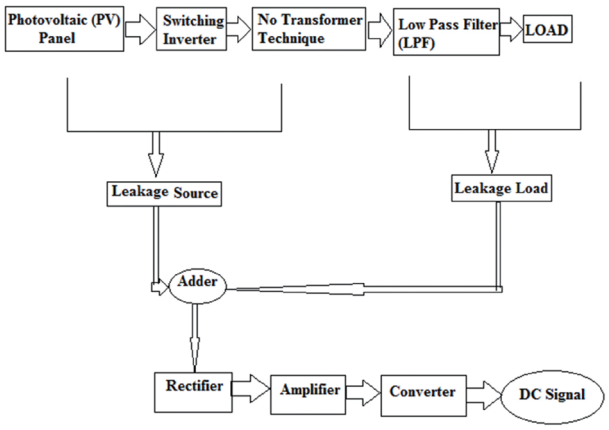

Fig. 1. System block diagram.

On the main power conversion path, the solar panel DC output is converted through a transformerless inverter to a chopped sine wave, powering a downstream resistive load. A higher-order low pass filter (HOLPFs) is used for filtering the output signal to a pure sine wave. On the harvesting signal path, the leakage currents are first summated to be further converted to a square-wave output. The obtained square-wave is passed through a low-pass filter for producing a sine wave. Subsequently, a rectifier circuit is used for converting the filtered signal to a quasi-DC output voltage. However, the existing voltage fluctuations are not a desirable feature for applications in DC output supplies. Thus, a flyback converter is used for converting the fluctuating signal to a stable DC output.

3. LEAKAGE CURRENT PATHS ANALYSIS

Figure 2 shows nine paths where the leakage current flows from different circuit nodes to ground through capacitive coupling. The waveforms for different the paths of the leakage current are shown below. The leakage current on the inverter side is shown with arrows

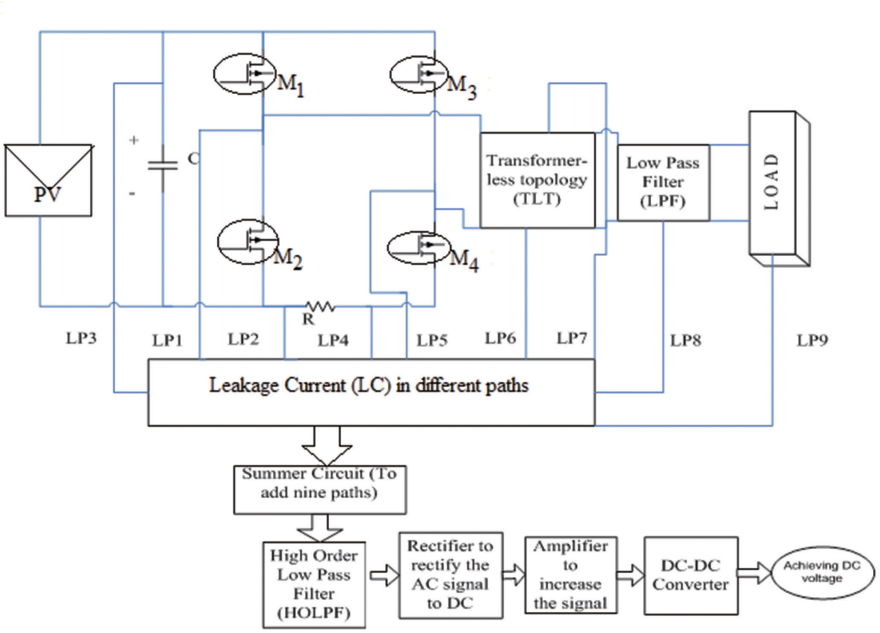

Fig. 2. Detailed schematic diagram.

when the switches are ON, while the other path has negligible currents. Meanwhile, the leakage current on the inverter side is zero during the OFF interval. The leakage current is also present in between the PV panel electrodes. However, the magnitude of the current remains in the picoampere range. The leakage current between switches M_1, M_2 and M_3, M_4, respectively, has been shown in Fig. 2. These two leakage paths are present only for opposite switches' states. Moreover, the current waveforms for these two paths present as fluctuating sine wave of very low magnitude. In addition, the leakage paths are also shown on the two sides of the transformerless section components. These two paths exhibit fluctuating currents in the picoampere range.

The remaining two leakage paths are located from the load to ground. This current is negligible, flowing on both sides with a magnitude in the femtoampere range. On the other hand, before the low-pass filter input, the current waveform is similar to a sine wave with occasional fluctuations. Furthermore, the current between the HOLPF and ground is also negligible.

4. LEAKAGE CURRENT HARVESTING

The leakage currents thus collected can be used for producing a DC voltage large enough for driving light loads or charging their batteries. Hereby, ideal operating conditions are assumed under which the capacitances, resistances, and switches (MOSFET) are connected such that their parasitic effects or those due to their threshold voltage drops could be ignored. If not harvested, the resulting leakage current will be wasted. We will be taking into account only the leakage current, while ignoring the effects or influences of the external components (such as inductors, resistors, capacitors, switches, etc.) on the results, if any. Under ideal conditions, we assume X_L = 0.31416 Ω and X_C=3.1931 Ω for an inductor of 1 mH and a capacitor of 1 mF, respectively, at 50 Hz frequency.

There are shown five leakage current paths associated to the transformerless inverter, while the remaining four paths include those from the load, HOLPF, and transformerless block. The cutoff frequency for the HOLPF using a 0.1 mF capacitor and a 10 Ω resistor, (–3 dB attenuation) is 5,032.919 Hz for the third order filter. The high frequency components producing sharp signal transitions are thus attenuated. A parasitic capacitor of 1 nF and a load of 200 Ω were considered. Figure 2 also shows a resistance R = 10 kΩ between the two sides of the inverter.

Inverter side leakage equivalent circuit analysis:

The two leakage current paths from the inverter ground side being in a Δ-network configuration, were converted to an equivalent Y-network as shown in Fig. 3.

The positive half-cycle conduction path through the inverter is shown in Fig. 4.

During the positive half-cycle of the inverter, switches M_1 and M_4 are ON. The current path is shown in Fig. 4.

$$Z_{EQU(+)} = [(5000 + 3183 * 10^6) \parallel (200 + 5000)] + 1 = 5.2\ \text{k}\Omega \quad (1)$$

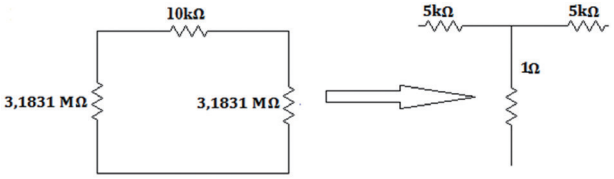

Fig. 3. Delta-to-Y conversion for impedance calculation.

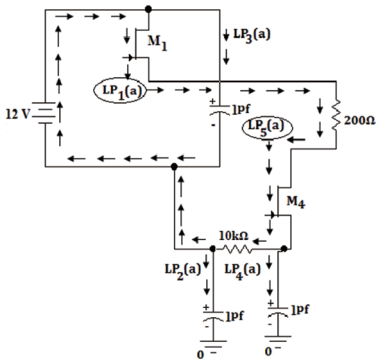

Fig. 4. Positive half-cycle path when switches M_1 and M_4 are ON.

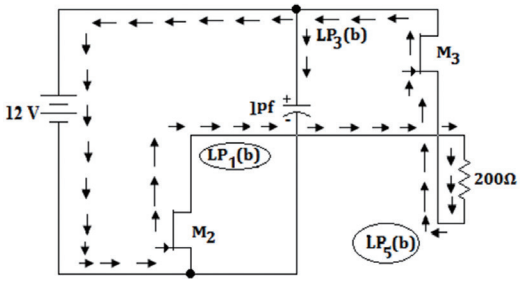

Fig. 5. Negative half-cycle path when switches M_3 and M_4 are ON.

$$I = \frac{12}{5201} = 2.31\ \text{mA} \quad (2)$$
$$LP_{1(a)} = 2.309\ \text{mA},\ LP_{5(a)} = 2.309\ \text{mA},$$
$$LP_{2(a)} = 37.4\ \text{pA},\ LP_{4(a)} = 0.235\ \text{nA, and}$$
$$LP_{3(a)} = 3.8\ \text{nA}$$

During the negative cycle of the inverter, switches M_3 and M_2 are ON. The current path is shown in Fig. 5.

$$Z_{EQU(-)} = 199.98\ \Omega \quad (3)$$
$$LP_{3(b)} = -14.5\ \text{nA},\ LP_{1(b)} = -2.308\ \text{mA},\ LP_{5(b)} = -2.308\ \text{mA}$$

The leakage currents for the five paths of the inverter are given below:

LP_1= 1 μA, LP_2 = 37.4 pA, LP_3= −18.3 nA, LP_4= −0.235 nA, and LP_5 = 1 μA.

Transformerless block analysis:

The transformerless technique consists in applying the H-bridge output voltage to a series of inductor-capacitor sections placed between the output of the inverter and load. The equivalent circuit diagram is shown in Fig. 6.

$$Z_{equ} = 1.9813\ \Omega \quad (4)$$
$$I = \frac{V}{Z_{equ}} = \frac{12 * 10^{-9}}{1.9813}$$
$$= 6.06\ \text{nA}$$
$$LP_6 = \frac{3.183 * 10^6 * 6.06 * 10^{-9}}{3.183 * 10^6 + 3.183 * 10^6} = 3.03\ \text{nA} \quad (5)$$
$$LP_6 = LP_7 = 3.03\ \text{nA}$$

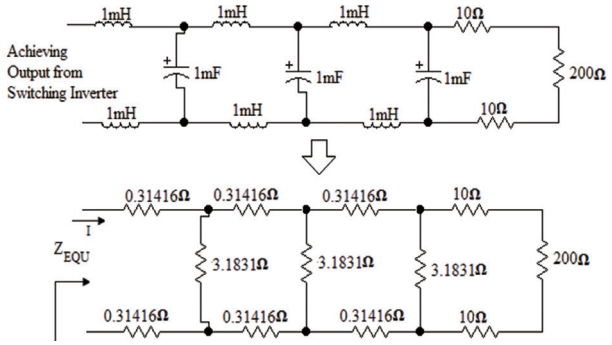

Fig. 6. Transformerless block equivalent impedance.

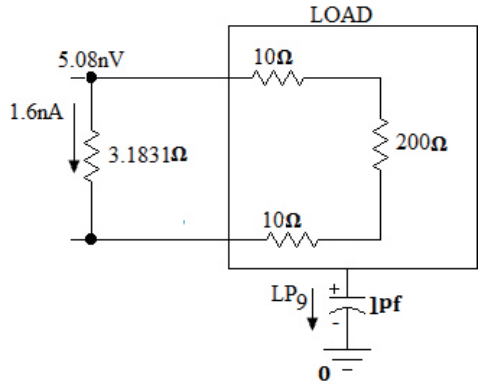

Fig. 7. Leakage current path on the load side.

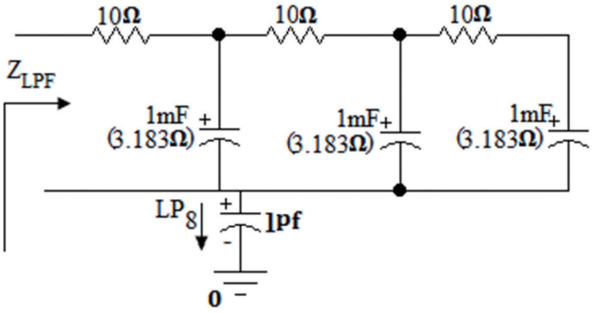

Fig. 8. Equivalent impedance for the third-order low pass filter.

The increase in input is due to the leakage current flowing through the two leakage paths.

Load and low pass filter (LPF) side equivalent circuit analysis:

The voltage at the output of the transformerless section is calculated to be 5.08 nV across an impedance of 3.1831 Ω, generating a current of 23.01 pA into a resistive load of 220 Ω and the current paths through load and HOLPF are shown in Fig. 7 and 8, respectively.

The leakage current for the filter (when connected) can be calculated from the load leakage current using the inverse-impedance proportional technique for current distribution, being given as:

In the above, we determined the currents from the nine leakage paths. To summate these currents, a non-inverting summing circuit with input-connected resistors was used.

5. RESULTS AND DISCUSSION

Leakage current occurs in inverters through parasitic capacitive coupling. This fluctuating current has become a concern in the grid-tied systems, increasing the power losses, maintenance costs, as well as decreasing the overall power efficiency. However, this fluctuating current can be converted to a useable form of energy. Hereby, it is presented a system where nine leakage current paths are identified in a transformerless inverter system with the purpose of leakage energy harvesting. A summation circuit is used to add the nine leakage currents for producing more than 1 V AC signal, further using a HOLPF to generate pure sine wave. A rectifier stage is used to convert the sine wave to a DC voltage.

The fluctuating DC voltage having an amplitude of around 1 V shown in Fig. 9 can be further stabilized by using a DC-DC converter.

In the above, the analytical expressions for the leakage currents flowing from the nine circuit nodes in a transformerless inverter connected to a PV panel system were shown. The total leakage current, ignoring the other external effects such as switching loss, capacitor loss, loss across the load, etc., is calculated as.

$$\begin{aligned} LI &= (LI\text{—}1 + LI\text{—}2 + LI\text{—}3 + LI\text{—}4 + LI\text{—}5 + LI\text{—}6 \\ &\quad + LI\text{—}7 + LI\text{—}8 + LI\text{—}9) \\ &= (1*10^{-6} + 37.4*10^{-12} - 18.3 * 10^{-9} - 0.235*10^{-9} + \\ &\quad 1*10^{-6} + 3.03*10^{-9} + 3.03*10^{-9} + 1.6*10^{-9} + 23.01 * 10^{-12}) \\ &= 1.989*10^{-6}\text{A} = 1.989\ \mu\text{A} \end{aligned}$$

Two types of MOSFET-based integrated rectifiers are used to perform the AC/DC conversion. The fully cross-coupled rectifier (FCCR) [17] yields an output voltage around 1 V when applying a sine wave of 1 V amplitude to its input. However, the gate cross-coupled rectifier (GCCR) output measured only around 600 mV under the same input conditions.

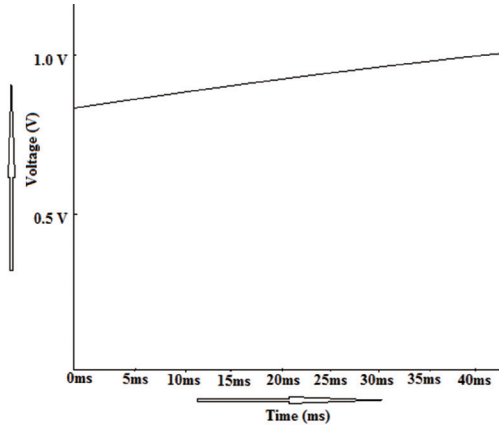

Fig. 9. Output voltage of the harvesting circuit.

While using the FCCR, a higher output voltage was achieved compared to using the GCCR. The FCCR was selected for its higher rectification performance and for solving the threshold voltage drop problem, since the GCCR could not [17].

6. CONCLUSIONS

Solar panels associated with inverters are increasingly used in the renewable energy field in larger installations as the rated power per PV module also increases. The PV system's DC voltage is converted to AC for injecting the generated power into the grid. The power

conversion core component in a solar-to-grid system is the inverter, mainly consisting of PWM-controlled switching devices configured in a certain topology. The transformerless topology has major advantages compared to the transformer-based topology. Although largely used for renewable AC generation, the transformerless topology also has a drawback related to leakage current. In this work is shown how the power losses associated to the leakage currents can be converted to a usable form of energy for low voltage battery charging purposes. Different leakage current paths are identified with the purpose of harvesting the leakage energy and generating a DC voltage. The leakage currents from a number of circuit nodes are collected, filtered, and rectified to produce a fluctuating DC voltage, which is further stabilized using a DC-DC converter. Employing a FCCR, the power transferred to a resistive load of 100.02 kΩ is shown to be in the milliwatt range. This amount of power is usable for supplying devices with low power requirements, also reducing power losses at the system level.

REFERENCES

[1] Y. Wang and J. Song, *Proc. 2012 Asia-Pacific Power and Energy Engineering Conference (APPEEC)* (IEEE, Shanghai, China, 2012) p. 1-4. [DOI: https://doi.org/10.1109/APPEEC.2012.6307188]

[2] R. F. Pantelimon, M. Adam, M. Andruşcă, and C. Pancu, *Proc. 2013 8th International Symposium on Advanced Topics in Electrical Engineering (ATEE)* (IEEE, Bucharest, Romania, 2013) p. 1-6. [DOI: https://doi.org/10.1109/ATEE.2013.6563367]

[3] S. B. Kjaer, J. K. Pedersen, and F. Blaabjerg, *IEEE Trans. Ind. Appl.*, **41**, 1292 (2005). [DOI: https://doi.org/10.1109/TIA.2005.853371]

[4] P. Phonrattanasak, M. Miyatake, and O. Sakamoto, *Proc. 2013 IEEE Energytech* (IEEE, Cleveland, USA, 2013) p. 1-6. [DOI: https://doi.org/10.1109/EnergyTech. 2013.6645334]

[5] N. S. Jamoshid, N. H. Hashim, R. B. Ali, and N. S. Saudin, *Proc. 2013 IEEE 7th International Power Engineering and Optimization Conference (PEOCO)* (IEEE, Langkawi, Malaysia, 2013) p. 139-143. [DOI: https://doi.org/10.1109/PEOCO.2013.6564531]

[4] L. Ma, F. Tang, F. Zhou, X. Jin, and Y. Tong, *Proc. 2008 IEEE International Conference on Sustainable Energy Technologies* (IEEE, Singapore, Singapore, 2008) p. 24-28. [DOI: https://doi.org/10.1109/ICSET.2008.4747018]

[5] A. Ravindranath, S. K. Mishra, and A. Joshi, *IEEE Trans. Power Electron.*, **60**, 5593 (2013). [DOI: https://doi.org/10.1109/TIE.2012.2230595]

[6] B. R. Lin and C. C. Chien, *IET Power Electron.*, **6**, 202 (2013).[DOI: https://doi.org/10.1049/iet-pel.2012.0127]

[7] M. J. Rani and S. Malarkkan, *Proc. International Conference on Sustainable Energy and Intelligent Systems (SEISCON 2011)* (IEEE, Chennai, India, 2011) p. 593–597. [DOI: https://doi.org/10.1049/cp.2011.0430]

[8] M.N.H. Khan, T. S. Gunawan, M. T. Rahman, and S. Khan, *Proc. 2014 International Conference on Computer and Communication Engineering* (IEEE, Kuala Lumpur, Malaysia, 2014) p. 269-272. [DOI: https://doi.org/10.1109/ICCCE.2014.83]

[9] M.N.H. Khan, K. J. Ahmad, M. S. Zahan, and M. N. Hasan, *International Journal of Power Electronics and Drive Systems (IJPEDS)*, **7**, 1193 (2016). [DOI: https://doi.org/10.11591/ijpeds.v7.i4.pp1193-1199]

[10] M.N.H. Khan, S. Khan, T. S. Gunawan, and R. I. Boby, *International Journal of Electrical, Computer, Energetic and Communication Engineering*, **9**, 1602 (2015). [scholar.waset.org/1999.5/10002660]

[11] A. Abdollahi, F. Fallah, and M. Pedram, *IEEE Transactions on Very Large Scale Integration (VLSI) Systems*, **12**, 140 (2004). [DOI: https://doi.org/10.1109/TVLSI.2003.821546]

[12] A. Abdollahi, F. Fallah, and M. Pedram, *IEEE Transactions on Very Large Scale Integration (VLSI) Systems*, **12**, 140 (2004). [DOI: https://doi.org/10.1109/TVLSI.2003.821546]

[13] M.N.H. Khan, S. Khan, T. S. Gunawan, and Z. Shahid, *Proc. 2013 IEEE International Conference on Smart Instrumentation, Measurement and Applications (ICSIMA)* (IEEE, Kuala Lumpur, Malaysia, 2013) p. 1-5. [DOI: https://doi.org/10.1109/ICSIMA.2013.6717970]

[14] M.N.H. Khan, K. J. Ahmad, S. Khan, and M. Hasanuzzaman, *International Journal of Power Electronics and Drive Systems (IJPEDS)*, **6**, 148 (2015). [DOI: https://doi.org/10.11591/ijpeds.v6.i1.pp148-159]

[15] M.N.H. Khan, S. Khan, T. S. Gunawan, and Z. Shahid, *Proc. 2013 IEEE International Conference on Smart Instrumentation, Measurement and Applications (ICSIMA)* (IEEE, Kuala Lumpur, Malaysia, 2013) p. 1-5. [DOI: https://doi.org/10.1109/ICSIMA.2013.6717931]

[16] Ó. López, F. D. Freijedo, A. G. Yepes, P. Fernández-Comesaña, J. Malvar, R. Teodorescu, and J. Doval-Gandoy, *IEEE Trans. Energy Convers.*, **25**, 140 (2010). [DOI: https://doi.org/10.1109/TEC.2009.2037810]

[17] H. Xiao, S. Xie, Y. Chen, and R. Huang, *IEEE Trans. Ind. Electron.*, **58**, 1887 (2011). [DOI: https://doi.org/10.1109/TIE.2010.2054056]

[18] P. Chaudhary and P. Sensarma, *IEEE Trans. Ind. Electron.*, **60**, 4359 (2013). [DOI: https://doi.org/10.1109/TIE.2012.2217724]

[19] M.N.H. Khan, M. T. Anower, K. J. Ahmad, M. M. Alam, M. S. Zahan, and M. H. Delwar, *Elixir Elec. Engg.*, **93**, 39574 (2016).

[20] S. S. Hashemi, M. Sawan, and Y. Savaria, *IEEE Trans. Biomed. Circuits. Syst.*, **6**, 326 (2012). [DOI: https://doi.org/10.1109/TBCAS.2011. 2177267]

[21] N. H. Khan, *European Journal of Engineering Research & Science*, **1**, 43 (2016). [DOI: https://doi.org/10.24018/ejers.2016.1.1.15]

[22] M.N.H. Khan, M. T. Anower, M. D. Hossen, M. M. Alam, and K. J. Ahmad, *International Journal of Electrical and Computer Engineering*, **6**, 2025 (2016). [DOI: https://doi.org/10.11591/ijece.v6i5.10566]